

Beneficial Effects of Early mTORC1 Inhibition after Traumatic Brain Injury

Ina Nikolaeva,^{1,2} Beth Crowell,¹ Julia Valenziano,³ David Meaney,³ and Gabriella D’Arcangelo^{1,2}

Abstract

The mammalian target of rapamycin complex 1 (mTORC1) signaling pathway mediates many aspects of cell growth and regeneration and is upregulated after moderate to severe traumatic brain injury (TBI). The significance of this increased signaling event for recovery of brain function is presently unclear. We analyzed the time course and cell specificity of mTORC1 signal activation in the mouse hippocampus after moderate controlled cortical impact (CCI) and identified an early neuronal peak of activity that occurs within a few hours after injury. We suppressed this peak activity by a single injection of the mTORC1 inhibitor rapamycin 1 h after CCI and showed that this acute treatment significantly diminishes the extent of neuronal death, astrogliosis, and cognitive impairment 1–3 days after injury. Our findings suggest that the early neuronal peak of mTORC1 activity after TBI is deleterious to brain function, and that acute, early intervention with mTORC1 inhibitors after injury may represent an effective form of treatment to improve recovery in human patients.

Key words: controlled cortical impact; mTOR; rapamycin

Introduction

FOCUS ON THE STUDY of mild to severe traumatic brain injury (TBI) has increased in recent years and brought the attention of researchers and clinicians to the lack of available treatments for patients with such injury. Even mild, closed-head trauma to the brain can lead to temporary or permanent neurological symptoms, including epileptic seizures, behavioral changes, and impaired motor and cognitive function.^{1–3}

Negative consequences of TBI can arise from a combination of direct neuronal tissue damage, inflammatory response, and secondary excitotoxic damage.^{4,5} Spontaneous healing occurs, however, and in most cases leads to at least a partial recovery of brain function. To optimize recovery, it is therefore critical to understand which TBI-induced molecular events contribute to damage of the neuronal tissue and which promote healing. Understanding the nature of these mechanisms and their time course of induction will then allow us to develop potential therapeutic approaches to minimize damage and facilitate functional recovery of the injured brain.

Research has so far identified three main signaling pathways that are modulated by TBI *in vivo*: the Janus kinase-signal transducer and activator of transcription (JAK-STAT), phosphatidylinositol/protein kinase B [Akt]/mammalian target of rapamycin (PI3K/Akt/mTOR), and the mitogen-activated protein kinase (MAPK) pathways.⁶ The focus of the present study is on the PI3K/Akt/mTOR pathway, which other groups have shown to be strongly induced *in vivo* post-TBI.^{7,8}

The PI3K/Akt/mTOR signaling pathway is a major player in the control of cell size, dendrite and axon outgrowth during brain development, and repair.^{9,10} Growth factors and hormones typically stimulate this pathway through the activation of receptor tyrosine kinases, leading to the activation of the PI3K and downstream Akt, which in turn regulates the activity of many signaling molecules, including mTOR. This kinase forms two complexes, mTORC1 and mTORC2. mTORC1 activation specifically induces protein translation through activation of ribosomal protein S6 kinases and disinhibition of the transcription initiation factor eIF4E through phosphorylation of the inhibitor 4EBP1.¹¹

The role of this signaling pathway in TBI, however, is controversial. Indeed, studies have shown that both induction of PI3K activity by suppression of upstream inhibitor Pten and suppression of mTORC1 by the mTORC1-specific inhibitor rapamycin after TBI *in vivo* can have beneficial effects on recovery as measured by extent of tissue damage, motor function, neurological score, and learning and memory tasks in rodent models.^{12,13} These findings raise the question of whether PI3K/Akt/mTOR induction plays a dual role in the TBI sequelae by affecting different cell types at different time points after injury.

To address this issue, we examined the time course of PI3K/Akt/mTOR induction in the hippocampus after TBI in the whole tissue and at a cellular level, and discovered an early peak of mTORC1 activation that is specific to neurons. Further, we investigated the role of early mTORC1 activity using a single systemic injection of rapamycin in the immediate aftermath of the injury. We reasoned that

¹Department of Cell Biology and Neuroscience, ²Graduate Program in Molecular Bioscience, Rutgers, the State University of New Jersey, Piscataway, New Jersey.

³Department of Bioengineering, University of Pennsylvania, Philadelphia, Pennsylvania.

an early acute, short-term suppression of mTORC1 post-controlled cortical impact (CCI) best models the treatment a TBI victim might receive in an attempt to limit the extent of brain damage and promote recovery. Indeed we found that this simple treatment positively affects brain repair and promotes functional recovery, laying the foundation for further translational studies in TBI.

Methods

CCI

Adult C57BL/6 mice were anesthetized with isoflurane (5% induction, 2% maintenance in medical grade air: 21% oxygen, 78% nitrogen) and placed in a stereotaxic frame on a heating pad to maintain body temperature. A 4-mm diameter craniotomy was produced on the left parietotemporal region of the skull midway between bregma and lambda using a trephine (CMA7431058, Harvard Apparatus, Holliston, MA), rotating the trephine by hand to advance the cutting blade through the skull. The area was cleaned periodically with saline during the procedure to rinse away bone fragments from the injury site. No overt bleeding was observed in the underlying cortex. Isoflurane was stopped 30 sec before CCI.

A moderate CCI was produced at a velocity of 2.4 m/sec with an impact depth of 1.15 mm, centering the impact at approximately -2.5 mm bregma. In a control group (sham), animals underwent craniotomy, placed in the stereotaxic holder, but no CCI was delivered. Anesthesia was reinstated after injury, and the exposed area was sutured closed. After surgical closure, mice were allowed to emerge from anesthesia and placed in a heated cage to wake and recover.

At different time points after injury (1, 2, 4, 8, 24 h or 7 days), animals were euthanized and processed for either immunohistochemistry or Western blot analysis. For immunohistochemistry, mice were transcardially perfused with 30 mL of ice-cold phosphate-buffered saline (PBS) (pH 7.4) and then with 40 mL of ice-cold 4% paraformaldehyde. Brains were harvested, post-fixed overnight in 4% paraformaldehyde at 4°C, and then cryoprotected in 24% sucrose. For Western blotting, brains were dissected and the hippocampi separated into lesion-side (L-side, experimental injury sample) and contralateral-side (C-side, internal control sample). The tissue was flash frozen in liquid nitrogen within 3 min of extraction for Western blot analysis.

Drug treatments

Mice in four treatment groups were sacrificed at time points specified in parenthesis: 25 rapamycin treated injured (2, 4, 8, and 24 h, $n=4-9$ mice per time point), 25 vehicle treated injured (2, 4, 8, and 24 h, $n=4-9$ mice per time point), 25 rapamycin treated sham (2, 4, 8, and 24 h, $n=4-8$ mice per time point), 24 vehicle treated sham (2, 4, 8, and 24 h, $n=4-8$ mice per time point). One hour post-CCI or sham, mice were injected intraperitoneally with either rapamycin (Calbiochem®) or vehicle (5% polyethylene glycol [PEG], 5% Tween-80 in saline) at a dose of 1 mg/kg of body weight. We selected this dose based on past studies¹³ and our preliminary dose-response studies. All experiments and animal housing were in accordance with procedures approved by the Animal Care and Use Committees at both University of Pennsylvania and Rutgers University, according to the National and Institutional Guidelines for Animal Care established by the National Institutes of Health.

Western Blot analysis

Hippocampal tissue was freshly dissected from the L-side and the C-side of the brain after CCI or sham injury, and lysed in radioimmunoprecipitation (RIPA) buffer (50 mM Tris pH 7.4, 1% NP40, 0.25% sodium deoxycholate, 150 mM NaCl, 1 nM ethylenediaminetetraacetic acid [EDTA] supplemented with protease and

phosphatase inhibitors). The tissue was homogenized and spun at 4°C, at 3000 rcf for 5–7 min to remove debris, and protein concentration was measured by a standard Bradford assay. Laemmli sample buffer was added to the lysates, and the samples were boiled for 3 min.

Proteins (20 µg per sample) were separated by SDS-PAGE using 8.0% or 10.0% gels and transferred onto 0.2 µm nitrocellulose membrane at 4°C in 20% methanol Tris-Glycine buffer for 2.5 h at a constant 0.5 Amp. Membranes were blocked in 3% milk in TBS-T for 1 h, and incubated in primary antibodies overnight at 4°C. Membranes were then incubated for 1 h in secondary horseradish peroxidase (HRP)-conjugated antibodies, and subjected to ECL-Plus Western Blotting Detection System (Pierce/Thermo Fisher, Rockland, IL). Primary antibodies against phospho-ribosomal protein S6 (Ser235/236) (pS6), phospho-Akt (Thr308) (pAktT), total Akt, and S6 were purchased from Cell Signaling, and anti-actin antibody was purchased from Millipore.

All phosphorylated protein levels were normalized to the total amount of each protein. Quantification was performed using the band analysis function of Alpha Imager software (Protein Simple). For each condition, samples were analyzed from $n>3$ mice, average phosphorylated/total density values were calculated for each protein, and C-side values were set at 1. Statistical significance was calculated comparing L-side to C-side values using analysis of variance (ANOVA) and the *post hoc* Dunnett test. A *p* value of 0.05 or less was considered significant.

Immunofluorescence

Brains were frozen in a 30% sucrose/Cryo-OCT (optimum cutting temperature medium) compound solution (30:70 mixture; Fisher) and serially sectioned at 30–50 µm on a cryostat. Coronal slices were mounted directly on slides. Slides were thawed at room temperature, permeabilized in 0.1% Triton-X, and blocked in 5% normal goat serum (NGS). Slides were incubated with primary antibody in 5% NGS in 0.1% Triton-X overnight at 4°C. Slides were then washed in PBS, probed with fluorophore-conjugated secondary antibodies for 1 h at room temperature, and mounted in Vectashield Mounting Medium with DAPI (Vector Laboratories). The following antibodies were used: Fluorophore-conjugated AlexaFluor 488-anti-pS6 (Ser235/236) (1:250, Cell Signaling Technology), anti-gial fibrillary acidic protein (GFAP) (1:250, Cell Signaling Technology or 1:500, Dako), anti-NeuN (1:100, Millipore), and anti-Iba1 (1:250, Wako).

Multiple sections from 3–4 mice per treatment were examined at each time point. Representative images were acquired using a Yokogawa CSU-10 spinning disk confocal head attached to an inverted fluorescence microscope (Olympus IX50), or an epifluorescence microscope (Olympus BX3-CBH). Positive cell counts were performed manually and in blind. Statistical significance in positive cell number was determined by the Student *t* test when only two datasets were compared, or by ANOVA and the Dunnett *post hoc* analysis for more than two datasets. $p<0.05$ was considered significant.

Fluoro-Jade B staining

Slides were washed in PBS to remove OCT, then washed in TBS and dried. Dried tissue was serially washed in 1%NaOH and 80% alcohol, 70% alcohol, DI, 0.06% KMnO₄, and DI. Slides were incubated in Fluoro-Jade B (FJB) staining solution (4% FJB, Millipore, in acetic acid) for 20 min. Slides were then washed in distilled water, dried, washed in xylene and mounted in DPX (VWR). Representative images were acquired using a Yokogawa CSU-10 spinning disk confocal head attached to an inverted fluorescence microscope (Olympus IX50).

Because FJB staining did not allow us to distinguish and count individual positive cells, an analysis of the fluorescence intensity was performed using ImageJ. Fluorescence analysis for hippocampal

areas, such as dentate gyrus (DG) and CA3, was performed by measuring the integrated density of the cell body layer after subtracting the background (area \times mean gray value of adjacent background). Intensity values were normalized to the selected areas to obtain corrected total fluorescence values. Comparison between these values obtained from vehicle- versus rapamycin-treated brains was performed using the Student *t* test. $p < 0.05$ was considered significant.

Morris water maze

Three days post-injury, spatial learning and memory were tested using the Morris water maze.¹⁴ A standard Morris water maze tank configured for mice was used for all assessments. A metal tank, 1 m in diameter, was painted flat black. A removable platform made of clear Plexiglas (10 cm in diameter) was placed in the southeast quadrant of the pool (in accordance with Smith and associates¹⁴). The pool was filled with water (22–26°C) to a level 1 cm above the platform surface. Nontoxic white Prang tempera paint (Prang and Dixon Ticonderoga, Heathrow, FL) was added to the water to mask the platform location and increase the visual contrast between the mouse and background. Visual cues consisted of laminated construction paper of varying shades and shapes taped to the inside walls of the pool, approximately 3 inches above the water line.

The start location of the mice was rotated among four directions (North, South, East, and West), and the time for the mouse to reach the platform was recorded. Mice were removed from the pool on climbing onto the platform. Animals that failed to find the platform were assigned a maximum score of 90 sec. Between trials, mice were placed in their home cages under heat lamps and allowed to rest for at least 10 min. For each animal, we used a single block of eight consecutive trials, equally spaced over the 8 h testing period. The average time to the platform (latency) for the last four trials was reported as the average latency to platform. To assess whether CCI or rapamycin caused compounding motor effects, swim speed was measured for vehicle- or rapamycin-treated animals in naïve, sham, and CCI groups. Statistical significance was calculated using ANOVA. p value < 0.05 was considered significant.

Statistics for behavioral tests

All statistical tests were performed using a commercially available statistical software package (JMP Pro, v. 11, Cary, NC). We used a mixed model to consider the fixed effects (treatment \times injury) and the repeated measures (trials) of the experimental design. We used the mixed model structure to evaluate the latency times over consecutive trials in the first half (trials 1–4) and second half (trials 5–8), consistent with previous work.¹⁵ If the mixed model produced significant differences for the fixed effects measures and/or their interaction across these two trial groups, we then used the Tukey honest significant difference (HSD) testing for *post hoc* comparison.

Results

Time course of CCI-induced PI3K/Akt/mTOR activity in the lesioned hippocampus

Adult C57Bl6 mice underwent moderate CCI or sham injury and were allowed to recover for 1, 2, 4, 8, 24 h or 7 days before brain dissection and protein extraction. CCI caused extensive tissue damage to the cerebral cortex on the L-side of the brain, but the hippocampus was relatively spared (Fig. 1D). Therefore, the effect of the CCI injury on the PI3K/Akt/mTOR pathway (Fig. 1A) was analyzed only in this tissue. No damage of the cerebral cortex or hippocampus in the C-side of the brain was observed (Fig. 1D).

To minimize variability inherent in the use of multiple mice and multiple blots, we measured signaling activity comparing L-side values with C-side values (set at 1) by Western blotting.

Phospho-specific antibodies against pAktT (Thr308, a readout of PI3K activity) and pS6 (Ser235/236, a readout of mTORC1 activity) were used to probe the activity of the signaling pathway. Levels of phosphorylated proteins were normalized to total levels of proteins in $n > 4$ mice per time point.

Levels of pAktT were found to be significantly higher in the L-side than in the C-side of the hippocampus only at 2 h post-CCI and returned to normal by 8 h (Fig. 1B,C). We also analyzed levels of pAkt (Ser473), a site targeted by mTORC2 and not strictly dependent on PI3K activity, but found no significant induction at any time point (data not shown). Levels of pS6, on the other hand, were significantly higher in the L-side over a broad period (2–8 h) post-CCI and returned to lower levels at later time points (Fig. 1B,C). Levels of CCI-induced pS6 peaked by 3–4 fold between 2 and 4 h in the L-side hippocampus.

No induction of PI3K/Akt/mTOR pathway was observed in the hippocampus in response to sham craniotomy at any time point analyzed (Fig. 1C and data not shown). Craniotomy alone did cause activation of the PI3K/Akt/mTOR pathway in the L-side cerebral cortex, even though there was no evidence of tissue damage resulting from craniotomy during perfusion, sectioning, or immunostaining (data not shown). Given the sham effect, and the extensive damage to this region resulting from CCI, the cerebral cortex was not analyzed further.

Immunofluorescence experiments using a fluorophore-conjugated anti-pS6 antibody confirmed extensive phosphorylation of this mTORC1 target in the cell body layers of areas CA1, CA3, and DG in the L-side hippocampus 4 h after CCI (Fig. 1F). The organization of these cellular layers appeared somewhat disrupted by the injury; however, individual pS6-positive cells were readily observed. The pS6 signal was completely absent from similar regions of the C-side hippocampus, in which the cell body layers appeared intact (Fig. 1F). Together, these studies demonstrate a modest activation of PI3K/Akt and a robust, but transient activation of mTORC1 in the injured hippocampus within a few hours after CCI.

Early mTORC1 activation in the injured hippocampus occurs in neuronal cells

To determine which cell types undergo mTORC1 activation within a few hours post-CCI in the L-side hippocampus, we conducted double immunofluorescence using fluorophore-conjugated anti-pS6 (Ser235/236) antibody in conjunction with a cell type-specific antibody, such as the neuronal marker NeuN or microtubule-associated protein 2 (MAP2), the astroglial marker GFAP, and the microglial marker Iba1. All four markers reliably label the expected cell types in the mouse hippocampus.

Sections obtained from mice sacrificed 4 h post-CCI revealed that only some neuronal cells, identified by either NeuN or MAP2 labeling, expressed high levels of pS6 in the cell body layers of area CA1 (Fig. 2A,B), CA3, and DG (data not shown). GFAP and Iba1 signals did not colocalize with pS6 in any hippocampal region (Fig. 2C,D). These data demonstrate that the early activation of mTORC1 in the injured hippocampus occurs specifically in a subset of neuronal cells within the cell body layers of the hippocampus.

A single rapamycin injection post-CCI suppresses injury-induced mTORC1 activity

To study the significance of mTORC1 activation in CCI-induced tissue damage and recovery, we injected mice with the mTORC1 inhibitor rapamycin one time at 1 h post-injury. This single injection method was used to determine whether it may be beneficial,

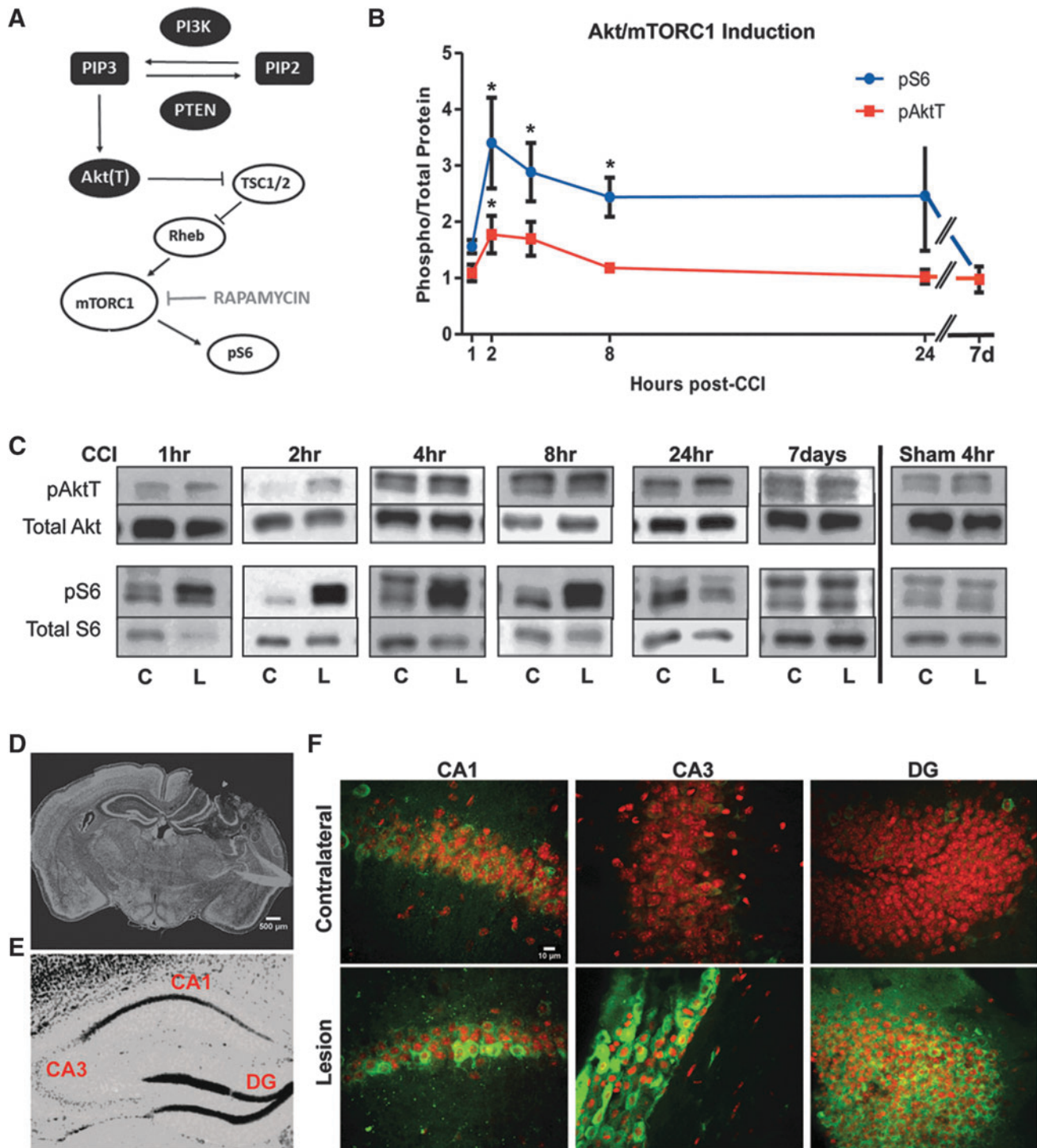


FIG. 1. Induction of the Akt/mTORC1 signaling pathway by controlled cortical impact (CCI). **(A)** Diagram of the PI3K/Akt/mTORC1 signaling cascade. **(B)** Time course of phosphorylation of Akt (pAktT) and S6 (pS6) proteins in the hippocampus after CCI. Values indicate the average ratio of phosphorylated/total proteins in the lesion side relative to the contralateral side of each injured brain (* $p < 0.05$ by analysis of variance). **(C)** Representative Western blot data showing the levels of phosphorylated and total Akt and S6 proteins at each time point in the lesion (L) and contralateral (C) side after CCI or sham surgery. **(D)** Representative low magnification image of a whole brain section after CCI. The section was stained with SYTOX nuclear stain. **(E)** Sample image of the hippocampus showing the location of regions of interest, such as area CA1, CA3, and dentate gyrus (DG). **(F)** High magnification (20x) confocal images of the CA1, CA3, and DG regions in the C and L side of the brain after CCI. Sections were stained with fluorophore-conjugated anti-pS6 antibody (green) and Reddot 2 nuclear stain. Scale bars: 500 μm (D) and 10 μm (F). Color image is available online at www.liebertpub.com/neu

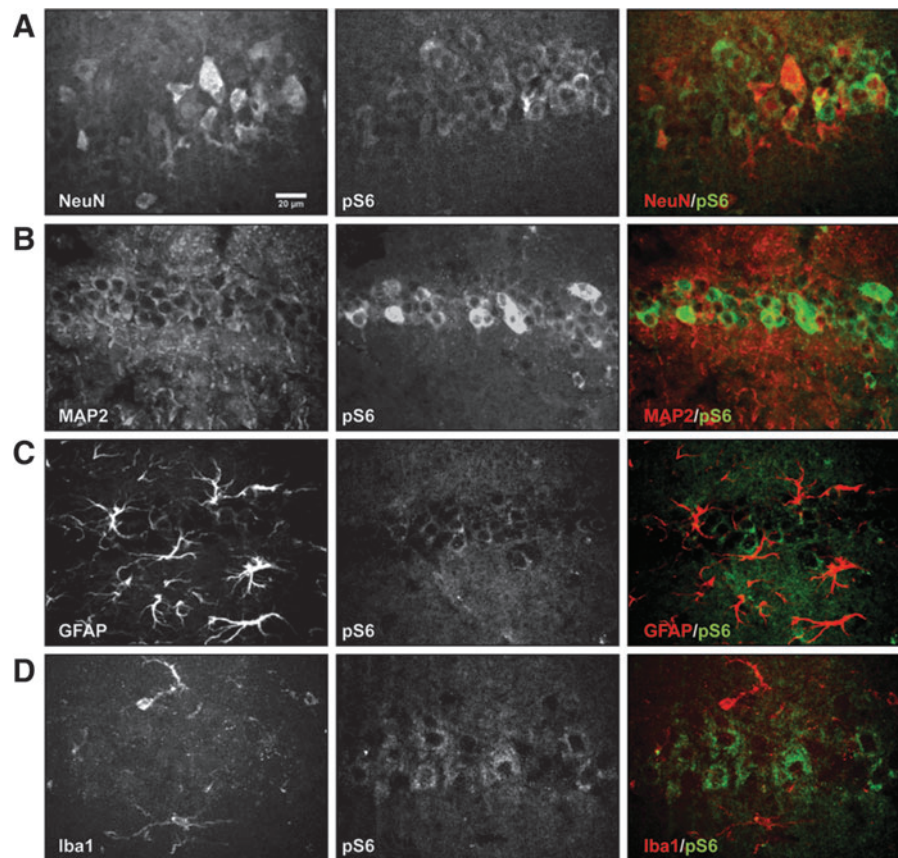


FIG. 2. Neuron-specific activation of mTORC1 signaling by controlled cortical impact (CCI). High magnification (20x) confocal images of the CA1 hippocampal area in the lesion side of the brain 4 h post-CCI. Sections were double labeled with antibodies against pS6 (green) and cell specific markers (red) such as neuronal markers NeuN (A) or microtubule-associated protein 2 (MAP2) (B), astroglia marker glial fibrillary acidic protein (GFAP), (C), and microglia marker Iba1 (D). Images are representative of data obtained in $n=3$ mice. Only neuronal markers colocalized with pS6. Scale bar: 20 μm for all panels. Color image is available online at www.liebertpub.com/neu

modeling a possible strategy for intervention in patients after TBI. Because rapamycin is a potent drug that lingers in the brain for a prolonged period,¹⁶ we reasoned that an early single injection may be sufficient to suppress the observed transient induction of mTORC1 and to elicit beneficial results, avoiding common side effects associated with prolonged, multi-day treatments with this drug.^{17,18}

Adult mice underwent the same moderate CCI described above and were injected once intraperitoneally with 1 mg/kg rapamycin or vehicle control 1 h after injury. Different cohorts of injected mice were sacrificed at 4 h post-CCI to assess the effect of the drug on signal transduction, at 24 h to examine cell damage and astrogliosis, or were analyzed at 3 days for cognitive function (Fig. 3A). At 4 h post-CCI, Western blot analysis of hippocampal tissue revealed that pS6 levels were strongly elevated (by approximately 4-fold) in vehicle-treated mice (Fig. 3B,C), similar to previously analyzed untreated mice (Fig. 1B,C).

Rapamycin treatment strongly suppressed this activation, resulting in L-side pS6 levels that were similar to sham controls (Fig. 3B,C). Even though a modest increase in pS6 levels was detected in rapamycin-treated mice when L-side samples were directly compared with C-side values ($p < 0.05$ by Student *t* test), statistical analysis of the whole data set, including sham-treated and vehicle-treated mice, indicated that only the L-side samples of vehicle-treated CCI-exposed mice exhibited significantly elevated levels of pS6 ($p < 0.05$ by ANOVA).

Interestingly, rapamycin treatment also caused a modest induction of pAktT levels in the L-side versus the C-side hippocampus (Student *t* test, $p < 0.05$) (Fig. 3B,D). This likely reflects a positive feedback mechanism that attempts to compensate for the downstream loss of mTORC1 signaling activity.^{19,20} A very small and not statistically significant induction of pAktT was also seen in vehicle-treated mice (Fig. 3B,D), similar to untreated samples previously analyzed at 4 h post-CCI (Fig. 1B). When the whole pAktT data set was analyzed by ANOVA, however, no significant effect of any of the treatments was found in either the L-side or the C-side of the hippocampus ($p > 0.05$) (Fig. 3D).

To confirm the effectiveness of the rapamycin injection on mTORC1 activity, we also conducted immunofluorescence experiments using a fluorophore-conjugated pS6 antibody. As previously noted for untreated mice (Fig. 1,2), pS6 levels were strongly induced 4 h post-CCI in the L-side of vehicle-treated mice in many pyramidal cells of area CA1 (Fig. 3E), as well as in cellular layers of area CA3 and DG (not shown). Rapamycin treatment dramatically suppressed pS6 immunoreactivity in these hippocampal regions (Fig. 3E and data not shown).

Levels of mTORC1 activity were further assessed by counting the number of pS6-positive cells per random field of view in the cell body layers of areas CA1, CA3, and DG in the L-side hippocampus. The number of pS6-positive cells was significantly reduced in rapamycin-treated compared with vehicle-treated mice (Fig. 3F)

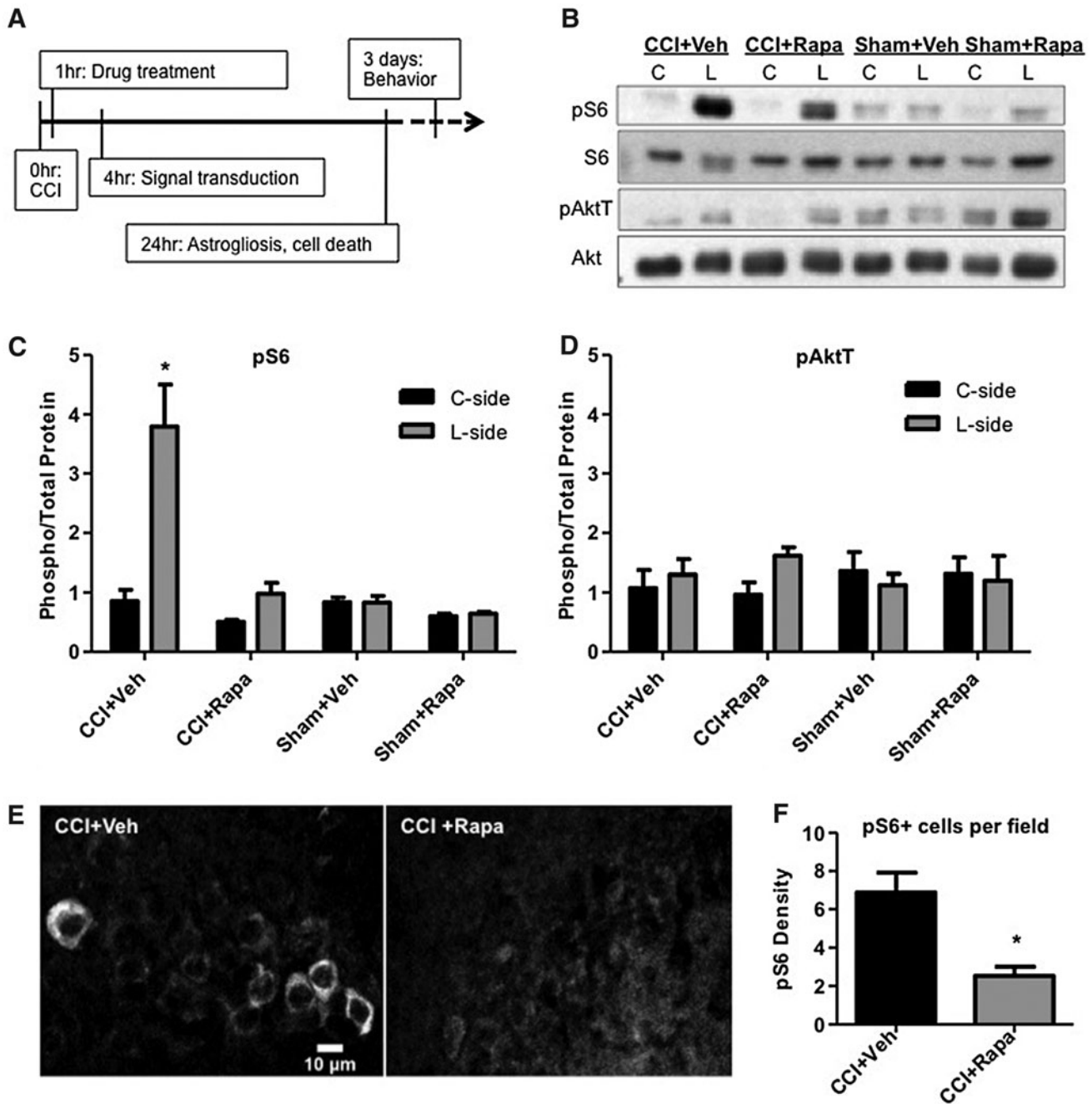


FIG. 3. Inhibition of mTORC1 signaling by rapamycin. **(A)** Schematic of the timeline of drug treatments and biological processes analyzed after controlled cortical impact (CCI). **(B)** Western blot analysis of normalized pAktT and pS6 levels in the lesion (L) and contralateral (C) side of the hippocampus in vehicle- (Veh) or rapamycin-treated (Rapa) mice 4 h post-CCI or sham surgical procedure. Quantification of pS6 **(C)** and pAktT **(D)** data. Values indicate the average ratio of phosphorylated/total proteins relative to the contralateral side (C-side) of CCI+Veh samples. CCI induced statistically significant pS6 levels only in Veh-treated, but not in Rapa-treated mice ($*p < 0.05$ by analysis of variance and *post hoc* analysis by Dunnett test). **(E)** Immunofluorescence analysis of pS6 levels in area CA1 of the L-side of the brain 4 hr post-CCI in Veh- or Rapa-treated mice. **(F)** Quantification of the number of pS6-positive cells per field of view in the pyramidal layer of area CA1. Rapa significantly suppresses pS6 induction by CCI ($*p < 0.05$ by Student *t* test). Scale bar: 10 μ m.

(Student *t* test, $p < 0.05$). No induction of pS6 was detected in the C-side hippocampus of injured rapamycin- or vehicle-treated mice (data not shown). Together, our Western blot and immunofluorescence data demonstrate that a single rapamycin injection delivered 1 h after CCI effectively suppresses mTORC1 activity in the injured hippocampus.

Rapamycin injection post-CCI reduces tissue damage in the injured hippocampus

To evaluate the effects of the single rapamycin treatment on hippocampal tissue damage, we stained brain sections collected 24 h post-CCI with FJB. This time is a recognized early point at

which post-CCI deficits can be observed and is optimal for FJB signal detection in the DG and CA3, but not in the CA1 area.^{21,22} FJB staining is specific for damaged neurons and has been used as a reliable method to quantify post-CCI damage in the L-side of the brain.²³ Indeed, we detected extensive FJB signal in the L-side and no detectable signal in the C-side hippocampus of vehicle-treated CCI-exposed mice in low magnification images (Fig. 4A).

To analyze tissue damage in more detail, we collected higher magnification images of hippocampal regions CA1, CA3, and DG in both vehicle- and rapamycin-treated mice that had been exposed to CCI. The FJB signal was limited to very few cells in the CA1 region of both treatment groups, as expected for the 24 h time point,²² and this area was therefore not analyzed further (Fig. 4B). In both CA3 and DG, extensive FJB staining was observed in all samples, although the signal appeared reduced in rapamycin-treated compared with vehicle-treated mice (Fig. 4B). Since individual cells could not be easily distinguished, an analysis of the FJB fluorescence signal was performed in the cellular layers of the CA3 and DG. The mean fluorescence signal was significantly reduced in rapamycin-treated compared to vehicle-treated mice in both hippocampal regions (Fig. 4C,D). The data demonstrate that acute rapamycin treatment post-CCI reduces the extent of tissue damage in the injured hippocampus.

Rapamycin injection post-CCI reduces astrogliosis in the injured hippocampus

We examined the effects of CCI and rapamycin treatment on hippocampal astrogliosis by staining sections collected at the 24 h

time point with the astroglial marker GFAP. Low-power images of the whole hippocampus revealed that CCI induces extensive astrogliosis in the C-side (Fig. 5B) as well as the L-side hippocampus (not shown), whereas sham operation did not have any effect (Fig. 5B). Western blot analysis confirmed an increase in GFAP expression in both the C-side and L-side hippocampus of CCI-exposed mice compared with sham-exposed controls (Fig. 5A). CCI-induced astrogliosis was limited to the hippocampus proper areas CA1 and CA3 and did not involve the DG (Fig. 5B). Therefore, these areas were further analyzed in higher magnification images.

In area CA1 (Fig. 5D), astrogliosis was present in vehicle-treated CCI-exposed mice in the C-side and was especially strong in the L-side. Rapamycin reduced astrogliosis in both sides of the hippocampus. The C-side of rapamycin-treated mice appeared indistinguishable from a sham control (Fig. 5C,D), whereas the L-side showed an apparent, but partial improvement compared with vehicle-treated sections. Similar results were obtained when area CA3 was analyzed (Fig. 5E,F).

To further quantify the effect of rapamycin treatment on astrogliosis we counted the number of GFAP-positive cells in random fields of area CA1 and CA3 in both the L-side and the C-side of the hippocampus. Statistical analysis indicated a significant reduction in the number of GFAP-positive cells in rapamycin-treated compared with vehicle-treated samples in both areas of the C-side (Student *t* test, $p < 0.05$) (Fig. 5G). The number of reactive astrocytes in the L-side, however, was not affected by the rapamycin treatment (data not shown). These data indicate that a single

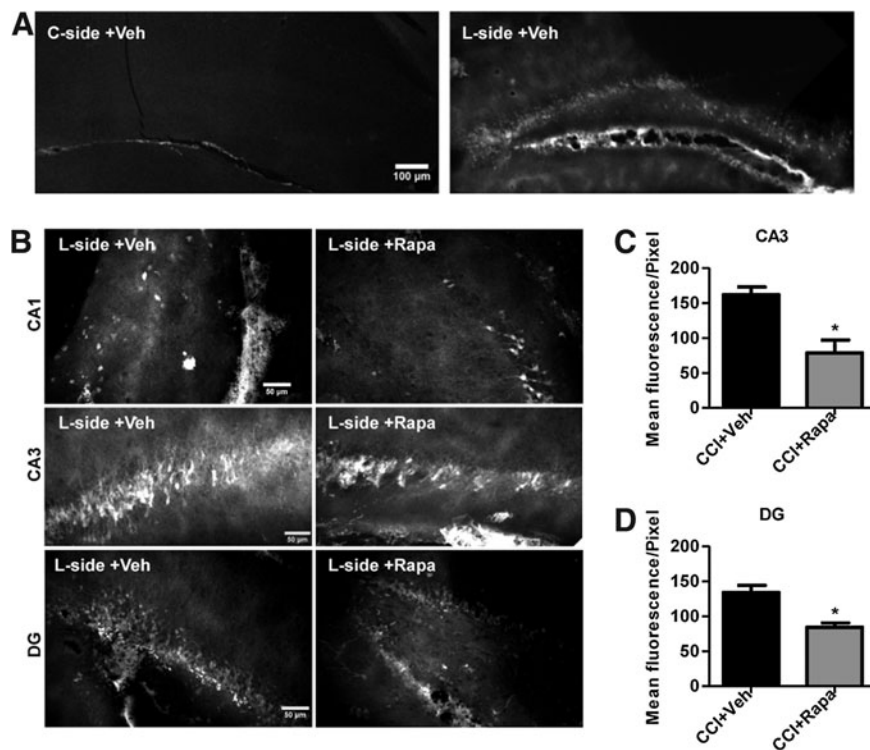


FIG. 4. Rapamycin reduces the extent of neuronal damage after controlled cortical impact (CCI). Mice were treated with vehicle (Veh) or rapamycin (Rapa), and analyzed 24 h after CCI. Sections were stained with Fluoro-Jade B and representative confocal images are shown. (A) Low magnification images of the hippocampus in the contralateral (C-side) and lesioned (L-side) hippocampus. (B) Higher magnification images of areas CA1, CA3, and DG in the L-side after Veh or Rapa treatment. Quantification of the Fluoro-Jade B signal in the pyramidal layer of area CA3 (C) and granule layer of the DG (D). Rapa treatment significantly reduced the number of damaged neurons in both areas ($*p < 0.05$ by Student *t* test). Scale bars: 100 μm (A) and 50 μm (B).

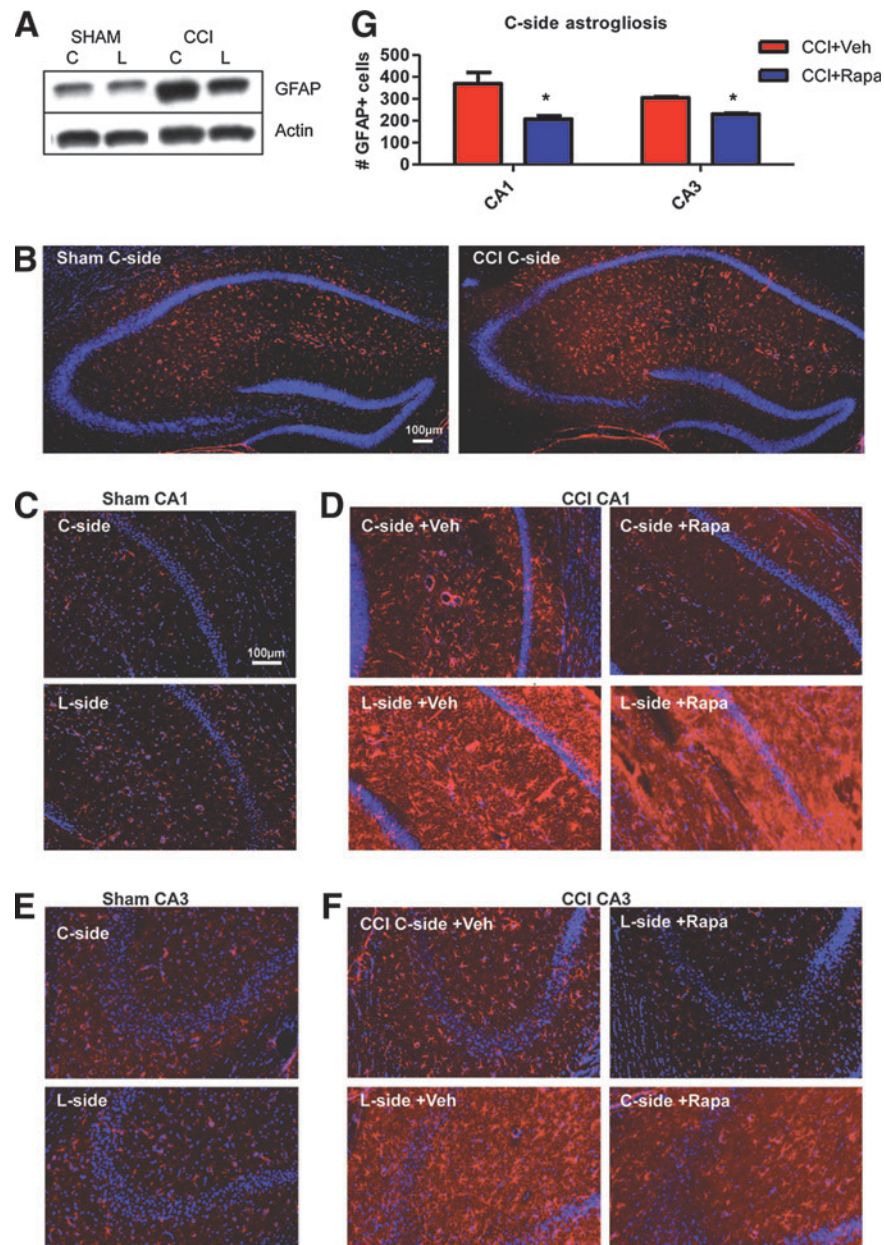


FIG. 5. Rapamycin suppresses astrogliosis after controlled cortical impact (CCI). Mice were treated with vehicle (Veh) or rapamycin (Rapa), and analyzed 24 h after CCI or sham surgery. Sections were stained with glial fibrillary acidic protein (GFAP) antibodies (red) and counterstained with 4',6-diamidino-2-phenylindole (DAPI) or Sytox (blue). (A) Western blot analysis of GFAP levels normalized to actin in the contralateral (C-side) or lesion side (L-side) after sham surgery or CCI. GFAP levels are elevated in both sides of the CCI-injured hippocampus. (B) Low magnification images of the C-side hippocampus after sham or CCI confirm the increase in the number of GFAP-positive cells after CCI. (C) Confocal images of area CA1 in the C-side or L-side after sham surgery. (D) Confocal images of area CA1 in the C-side or L-side after CCI and Veh or Rapa treatment. (E) Confocal images of area CA3 in the C-side or L-side after sham surgery. (F) Confocal images of area CA3 in the C-side or L-side after CCI and Veh or Rapa treatment. (G) Quantification of the number of GFAP-positive cells per area analyzed in the C-side of the brain in CA1 and CA3 regions. Rapa treatment significantly reduced astrogliosis in the C-side of both hippocampal areas ($*p < 0.05$ by Student *t* test). Scale bars: 100 μ m. Color image is available online at www.liebertpub.com/neu

rapamycin injection 1 h post-CCI can significantly reduce astrogliosis, particularly in the C-side of the hippocampus.

A single rapamycin injection partially rescues CCI-induced learning deficits

Given our findings that a single rapamycin injection 1 h after CCI suppresses mTORC1 activation, early neuronal degeneration, and

astrogliosis, we next tested whether this treatment also leads to amelioration of cognitive deficits after injury. Because of the acute nature of the changes in signaling after injury, we evaluated Morris water maze deficits 3 days after CCI (Fig. 6). The overall performance of the animals in acquiring the platform location calculated over the last four trials was significantly influenced by both injury and treatment: average latency times of sham-vehicle treated (14.9 ± 11.8 sec), sham-rapamycin treated (11.3 ± 9.3 sec), CCI-vehicle treated

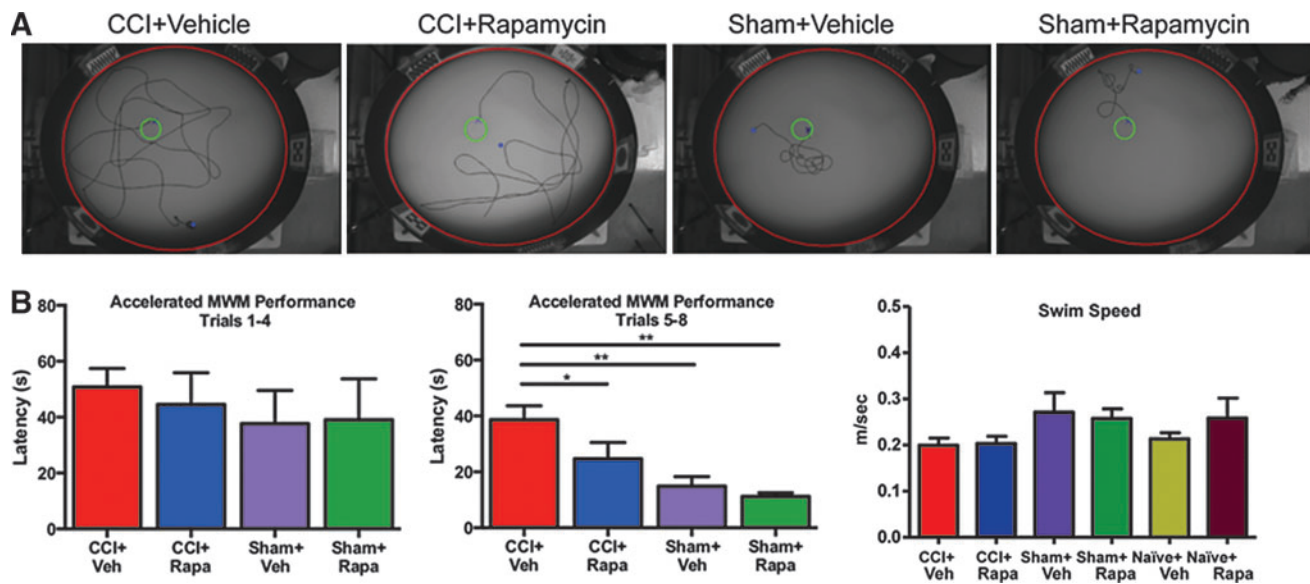


FIG. 6. Rapamycin treatment 1 h after injury improves cognitive function. Animals underwent moderate controlled cortical impact (CCI) injury (1.15 mm depth, 2.4 m/sec velocity) and were treated with a single intraperitoneal injection of rapamycin (1 mg/kg) 1 h after injury. Three days after injury, cognitive function was assessed using the Morris water maze (MWM), measuring latency to platform over a single block of eight equally spaced trials. (A) Representative trajectories of animals swimming to the platform in one of four categories were recorded. (B) Average latency times across the first four trial blocks did not differ. (C) Average latency times in the final four trials showed a significant effect of both injury and treatment (mixed linear model, $p < 0.05$). *Post hoc* testing showed that rapamycin (Rapa) treatment significantly improved latency to platform relative to vehicle (Veh) treated injured animals. (D) Average swim speed (m/sec) for naïve, sham, or CCI-injured animals treated with either Veh or Rapa (analysis of variance $p = 0.18$). Color image is available online at www.liebertpub.com/neu

(38.8 ± 21.6 sec), and CCI-rapamycin treated (22.7 ± 16.1 sec) animals showed significant effects of both injury ($p < 0.0001$) and treatment ($p < 0.0143$) and their interaction ($p < 0.022$).

Post hoc testing showed that significant performance differences were present between injured and sham animals receiving vehicle treatment ($p = 0.0001$), but that no differences were observed between sham injured animals receiving either vehicle or rapamycin treatment. Rapamycin treatment, however, significantly improved latency time in injured animals relative to vehicle treatment only after CCI injury ($p = 0.0061$), an improvement that was not apparent in sham animals ($p = 0.89$) (Fig. 6B). No difference in swim speed was observed between naïve-vehicle treated (0.21 ± 0.013), naïve-rapamycin treated (0.26 ± 0.043 m/sec), sham-vehicle treated (0.27 ± 0.042 m/sec), sham-rapamycin treated (0.26 ± 0.021 m/sec), CCI-vehicle treated (0.20 ± 0.016 m/sec), and CCI-rapamycin treated (0.20 ± 0.015 m/sec) animals ($p = 0.18$) (Fig. 6B).

Discussion

In this study, we analyzed the activity of the PI3K/Akt/mTOR signaling pathway in the adult mouse hippocampus after moderate CCI, and found a peak induction of mTORC1 activity at 2–8 h post-injury in the L-side of the brain, as evidenced by increased pS6 levels. We further showed that this activation is specific to neurons, which lose their tight layer organization in the injured hippocampus, and does not involve astrocytes or microglia. Previous work that examined the induction of pS6 levels 24 h post-injury indicated that signal activation occurs in glial cells as well as in neurons at this later time point.⁸

Thus, it appears that there is a shift in mTORC1 activation from neurons in the early hours after injury to glial cells at later times.

This delayed activation may result directly from injury to glial cells, indirectly from neuronal damage, or both. We reasoned that an early intervention with rapamycin 1 h post-CCI to suppress neuronal mTORC1 activation may reduce not only neuronal damage, but also prevent glial dysfunction at later stages. Indeed we found that this acute intervention strategy was beneficial in preventing both neuronal and glial abnormalities and improving functional recovery at least in the short term (3 days after injury).

Our results are consistent with a previous study that demonstrated neuroprotection, reduced microglial response, and improved behavioral performance when rapamycin was injected 4 h post-TBI.¹³ No beneficial effect on astrogliosis was seen in that study, however, nor in a study that administered rapamycin immediately before CCI.⁸ These studies, taken together with the data presented here, suggest that the most effective time window for an intervention that affects all cell types may be between 1 and 4 h post-TBI. This treatment paradigm would be applicable to at least some victims of TBI, because it allows a reasonable window of time for patients to be reached by medical personnel.

Previous work on TBI has produced conflicting evidence on the role of the PI3K/Akt/mTOR pathway in recovery from TBI. Unlike this study, some reports suggested that activation, rather than suppression, of the PI3K/Akt/mTOR pathway promotes recovery from TBI. In one study, long-term treatment with simvastatin beginning 24 h post-CCI, which stimulates Akt phosphorylation, was shown to stimulate neurogenesis and promote spatial learning after TBI.¹² In another, a single dose of rapamycin given just before the injury failed to improve cognitive performance as assessed by the Morris water maze using a CCI model, and worsened cognitive performance in a closed-head injury model.^{8,24}

Our findings are consistent with previous studies that demonstrate beneficial effects of mTORC1 signaling inhibition.^{13,24}

Interestingly, in these studies as in ours, rapamycin treatment was initiated in the 1 to 4 h window after injury. Thus, it is conceivable that the timing or the length of drug treatments targeting the Akt/mTOR pathway plays a significant role in determining recovery from TBI.

Rapamycin or rapalogs are widely used to suppress excessive mTORC1 activation in animal models of cortical malformations.^{25–29} In virtually all these models, rapamycin treatment not only significantly prolongs survival, prevents or suppresses neuronal abnormalities and glia pathology, but also strongly suppresses seizures. The overwhelmingly positive effects seen in animal studies led to the development of clinical trials to evaluate the effectiveness of rapalogs in the treatment of epilepsy in these developmental disorders.³⁰

On the other hand, few studies investigated the effects of rapamycin treatment in animal models of TBI. In one study, treatment was initiated 1 h post-TBI, but continued daily for several weeks, conferring not only protection from neuronal degeneration, but also preventing the development of post-traumatic epilepsy.²⁴ Together with our studies that demonstrated the beneficial effects of rapamycin on behavioral performance, this work suggests that mTORC1 inhibition may be a viable strategy to ameliorate several aspects of functional recovery after TBI.

As for all drugs, however, limitations for the use of rapamycin in the human patient population exist, and warrant caution in the interpretation of these findings. For example, the drug is known to confer nonspecific inhibition of other kinase complexes, such as mTORC2³¹ and produce considerable side effects in patients, especially when treatment is prolonged. These concerns, however, are attenuated if a strategy similar to that used in this animal study, consisting of a single, acute intervention shortly after TBI that is unlikely to cause adverse effects, would be applied to patients.

In this study, we showed that rapamycin delivered by systemic injection clearly entered the brain and suppressed the early neuronal phosphorylation of ribosomal protein S6 in the L-side hippocampus, indicating that the treatment successfully reduced mTORC1 activity in the injured brain. Both immunostaining and Western blotting data obtained at the 4 h time point after injury confirmed this result. By 24 h post-CCI, neuronal damage was extensive in the L-side, and astrogliosis was apparent in both sides of the injured brain, even though we observed no mTORC1 induction, cell damage, or cell body layer disruption in the C-side hippocampus.

Rapamycin treatment strongly reduced neuronal and astroglial pathology from CCI, suggesting that suppression of the early mTORC1 induction in the L-side was sufficient to reduce global astrogliosis. This suggests that early distress signals originating from neurons in the L-side of the brain may cause neuroinflammation in the C-side, and that these secondary effects of the injury may be completely preventable by early rapamycin intervention. Because we only saw a modest improvement of astrogliosis in the L-side in response to our acute rapamycin treatment, however, it is possible that repeated or additional forms of intervention are needed to fully prevent neuronal damage and neuroinflammation in the proximity of the injury.

Indeed, a previous study demonstrated that a combination therapy consisting of drugs that inhibit Akt, another kinase component of the PI3K/mTOR signaling pathway, as well as mTORC1 improves function outcome when applied before CCI.⁸ Further studies are needed, however, to determine whether such dual therapy is safe and effective in a clinically relevant post-TBI paradigm.

Conclusion

We demonstrate that CCI induces a deleterious activation of mTORC1 activity in hippocampal neurons, which then drives neuronal damage, widespread astrogliosis, and cognitive dysfunction. Early intervention with a single dose of rapamycin is greatly beneficial to reduce tissue damage and improve functional recovery, at least in the short term. Given these promising results, additional studies are warranted to investigate the long-term effects of single or intermittent acute rapamycin treatment on the sequelae of CCI. Future studies should also investigate the possible application of this intervention strategy to other animal models of TBI and to human patients.

Acknowledgments

This work is supported by multiprogrammatic grant CBIR12-MIG011 from the New Jersey Commission on Brain Injury Research (GD and DM).

Author Disclosure Statement

No competing financial interests exist.

References

- Okie, S. (2005). Traumatic brain injury in the war zone. *N. Engl. J. Med.* 352, 2043–2047.
- Kostyun, R.O., Milewski, M.D., and Hafeez, I. (2015). Sleep disturbance and neurocognitive function during the recovery from a sport-related concussion in adolescents. *Am. J. Sports Med.* 43, 633–640.
- Merritt, V.C., and Arnett, P.A. (2014). Premorbid predictors of post-concussion symptoms in collegiate athletes. *J. Clin. Exp. Neuropsychol.* 36, 1098–1111.
- Rose, M.E., Huerbin, M.B., Melick, J., Marion, D.W., Palmer, A.M., Schiding, J.K., Kochanek, P.M., and Graham, S.H. (2002). Regulation of interstitial excitatory amino acid concentrations after cortical contusion injury. *Brain Res.* 943, 15–22.
- Faden, A.I., Demediuk, P., Panter, S.S., and Vink, R. (1987). The role of excitatory amino acids and NMDA receptors in traumatic brain injury. *Science* 244, 798–800.
- Don, A.S., Tsang, C.K., Kazdoba, T.M., D'Arcangelo, G., Young, W., and Zheng, X.F. (2012). Targeting mTOR as a novel therapeutic strategy for traumatic CNS injuries. *Drug Discov. Today* 17, 861–868.
- Chen, S., Atkins, C.M., Liu, C.L., Alonso, O.F., Dietrich, W.D., and Hu, B.R. (2007). Alterations in mammalian target of rapamycin signaling pathways after traumatic brain injury. *J. Cereb. Blood Flow Metab.* 27, 939–949.
- Park, J., Zhang, J., Qiu, J., Zhu, X., Degterev, A., Lo, E.H., and Whalen, M.J. (2012). Combination therapy targeting Akt and mammalian target of rapamycin improves functional outcome after controlled cortical impact in mice. *J. Cereb. Blood Flow Metab.* 32, 330–340.
- Fingar, D.C., Salama, S., Tsou, C., Harlow, E., and Blenis, J. (2002). Mammalian cell size is controlled by mTOR and its downstream targets S6K1 and 4EBP1 / eIF4E. *Genes Dev.* 16, 1472–1487.
- Gong, R., Park, C.S., Abbassi, N.R., and Tang, S.J. (2006). Roles of glutamate receptors and the mammalian target of rapamycin (mTOR) signaling pathway in activity-dependent dendritic protein synthesis in hippocampal neurons. *J. Biol. Chem.* 281, 18802–18815.
- Laplante, M., and Sabatini, D.M. (2009). mTOR signaling at a glance. *J. Cell Sci.* 122, 3589–3594.
- Wu, H., Lu, D., Jiang, H., Xiong Y, Qu C, Li B, Mahmood A, Zhou D, and Chopp M. (2008). Simvastatin-mediated upregulation of VEGF and BDNF, activation of the PI3K/Akt pathway, and increase of neurogenesis are associated with therapeutic improvement after traumatic brain injury. *J. Neurotrauma* 25, 130–139.
- Erlich, S., Alexandrovich, A., Shohami, E., and Pinkas-Kramarski, R. (2007). Rapamycin is a neuroprotective treatment for traumatic brain injury. *Neurobiol. Dis.* 26, 86–93.
- Smith, D.H., Soares, H.D., Pierce, J.S., Perlman, K.D., Saatman, K.E., Meaney, D.F., Dixon, C.E., and McIntosh, T.K. (1995). A model of parasagittal controlled cortical impact in the mouse: cognitive and histopathologic effects. *J. Neurotrauma* 12, 169–178.

15. Choo, A.M., Miller, W.J., Chen, Y.C., Nibley, P., Patel, T.P., Goletiani, C., Morrison, B., 3rd, Kutzung, M.K., Firestein, B.L., Sul, J.Y., Haydon, P.G., and Meaney, D.F. (2013). Antagonism of purinergic signalling improves recovery from traumatic brain injury. *Brain* 136, 65–80.
16. Meikle, L., Pollizzi, K., Egnor, A., Kramvis, I., Lane, H., Sahin, M., and Kwiatkowski, D.J. (2008). Response of a neuronal model of tuberous sclerosis to mammalian target of rapamycin (mTOR) inhibitors: effects on mTORC1 and Akt signaling lead to improved survival and function. *J. Neurosci.* 28, 5422–5432.
17. Barlow, A.D., Xie, J., Moore, C.E., Campbell, S.C., Shaw, J.A., Nicholson, M.L., and Herbert, T.P. (2012). Rapamycin toxicity in MIN6 cells and rat and human islets is mediated by the inhibition of mTOR complex 2 (mTORC2). *Diabetologia* 55, 1355–1365.
18. Barlow, A.D., Nicholson, M.L., and Herbert, T.P. (2013). Evidence for rapamycin toxicity in pancreatic β -cells and a review of the underlying molecular mechanisms. *Diabetes* 62, 2674–2682.
19. Das, F., Ghosh-Choudhury, N., Dey, N., Mandal, C.C., Mahimainathan, L., Kasinath, B.S., Abboud, H.E., and Choudhury, G.G. (2012). Unrestrained mammalian target of rapamycin complexes 1 and 2 increase expression of phosphatase and tensin homolog deleted on chromosome 10 to regulate phosphorylation of Akt kinase. *J. Biol. Chem.* 287, 3808–3822.
20. Huang, J., and Manning, B.D. (2009). A complex interplay between Akt, TSC2, and the two mTOR complexes. *Biochem. Soc. Trans.* 37, 217–222.
21. Shein, N.A., Grigoriadis, N., Alexandrovich, A.G., Simeonidou, C., Spandou, E., Tsenter, J., Yatsiv, I., Horowitz, M., and Shohami, E. (2008). Differential neuroprotective properties of endogenous and exogenous erythropoietin in a mouse model of traumatic brain injury. *J. Neurotrauma* 25, 112–123.
22. Zhou, H., Chen, L., Gao, X., Luo, B., and Chen, J. (2012). Moderate traumatic brain injury triggers rapid necrotic death of immature neurons in the hippocampus. *J. Neuropathol. Exp. Neurol.* 71, 348–359.
23. Schmued, L.C., and Hopkins, K.J. (2000). Fluoro-Jade B: a high affinity fluorescent marker for the localization of neuronal degeneration. *Brain Res.* 874, 123–130.
24. Zhu, X., Park, J., Golinski, J., Qiu, J., Khuman, J., Lee, C.C., Lo, E.H., Degtarev, A., and Whalen, M.J. (2014). Role of Akt and mammalian target of rapamycin in functional outcome after concussive brain injury in mice. *J. Cereb. Blood Flow Metab.* 34, 1531–1539.
25. Kazdoba, T.M., Sunnen, C.N., Crowell, B., Lee, G.H., Anderson, A.E., and D’Arcangelo, G. (2012). Development and characterization of NEX- Pten, a novel forebrain excitatory neuron-specific knockout mouse. *Dev. Neurosci.* 34, 198–209.
26. Ljungberg, M.C., Sunnen, C.N., Lugo, J.N., Anderson, A.E., and D’Arcangelo, G. (2009). Rapamycin suppresses seizures and neuronal hypertrophy in a mouse model of cortical dysplasia. *Dis. Model Mech.* 2, 389–398.
27. Meikle, L., Talos, D.M., Onda, H., Pollizzi, K., Rotenberg, A., Sahin, M., Jensen, F.E., and Kwiatkowski, D.J. (2007). A mouse model of tuberous sclerosis: neuronal loss of Tsc1 causes dysplastic and ectopic neurons, reduced myelination, seizure activity, and limited survival. *J. Neurosci.* 27, 5546–5558.
28. Way, S.W., Rozas, N.S., Wu, H.C., McKenna, J., 3rd, Reith, R.M., Hashmi, S.S., Dash, P.K., and Gambello, M.J. (2012). The differential effects of prenatal and/or postnatal rapamycin on neurodevelopmental defects and cognition in a neuroglial mouse model of tuberous sclerosis complex. *Hum. Mol. Genet.* 21, 3226–3236.
29. Zeng, L.H., Xu, L., Gutmann, D.H., and Wong, M. (2008). Rapamycin prevents epilepsy in a mouse model of tuberous sclerosis complex. *Ann. Neurol.* 63, 444–453.
30. Krueger, D.A., Wilfong, A.A., Holland-Bouley, K., Anderson, A.E., Agricola, K., Tudor, C., Mays, M., Lopez, C.M., Kim, M.O., and Franz, D.N. (2013). Everolimus treatment of refractory epilepsy in tuberous sclerosis complex. *Ann. Neurol.* 74, 679–687.
31. Sarbassov, D.D., Ali, S.M., Sengupta, S., Sheen, J.H., Hsu, P.P., Bagley, A.F., Markhard, A.L., and Sabatini, D.M. (2006). Prolonged rapamycin treatment inhibits mTORC2 assembly and Akt/PKB. *Mol. Cell* 22, 159–168.

Address correspondence to:
Gabriella D’Arcangelo, PhD
Department of Cell Biology and Neuroscience
Rutgers, the State University of New Jersey
604 Allison Road, B323
Piscataway, NJ 08854
E-mail: darcangelo@dls.rutgers.edu